

# Synthesis and Structures of Bis[bis(trimethylsilyl)amido]-tin(IV) Cyclic Chalcogenides [ $\{\text{Sn}[\text{N}(\text{SiMe}_3)_2]_2(\mu\text{-E})\}_2$ ] and a Heterobimetallic Analogue [ $\{(\text{Me}_3\text{Si})_2\text{N}\}_2\text{Ge}(\mu\text{-Te})_2\text{Sn}\{-\text{N}(\text{SiMe}_3)_2\}_2$ ] (E = S, Se or Te)<sup>†</sup>

Peter B. Hitchcock, Eunseok Jang and Michael F. Lappert

*School of Chemistry and Molecular Sciences, University of Sussex, Brighton BN1 9QJ, UK*

Each of the four-membered ring compounds [ $\{\text{Sn}[\text{N}(\text{SiMe}_3)_2]_2(\mu\text{-E})\}_2$ ] (E = S 1, Se 2 or Te 3) has been prepared by the oxidative addition of the chalcogen E to  $\text{Sn}[\text{N}(\text{SiMe}_3)_2]_2$  promoted by sonication in a faster reaction and in a higher yield than previously achieved. The first heterobimetallic analogues [ $\{(\text{Me}_3\text{Si})_2\text{N}\}_2\text{Ge}(\mu\text{-E})_2\text{Sn}\{-\text{N}(\text{SiMe}_3)_2\}_2$ ] (E = Te 4 or Se 5) were obtained similarly from a mixture of the two metal(II) amides and the chalcogen. Compounds 1–4 have been characterised by single crystal X-ray diffraction and 1–5 studied by NMR spectroscopy [ $^1\text{H}$ ,  $^{13}\text{C}$ ,  $^{29}\text{Si}$ ,  $^{77}\text{Se}$ ,  $^{117}\text{Sn}$ ,  $^{119}\text{Sn}$ ,  $^{125}\text{Te}$  and (by the insensitive nuclei enhanced by polarization transfer technique)  $^{15}\text{N}$ ].

In Part 13,<sup>2</sup> the synthesis of bis[bis(trimethylsilyl)amido]-germanium(IV) and -tin(IV) chalcogenides [ $\{\text{M}[\text{N}(\text{SiMe}_3)_2]_2(\mu\text{-E})\}_2$ ] (M = Ge or Sn; E = S, Se or Te) by the thermal oxidative-addition reaction between bis[bis(trimethylsilyl)amido]-germanium(II) or -tin(II) and an elementary chalcogen was described. Previously<sup>3</sup> it had been shown that  $\text{Ge}[\text{N}(\text{SiMe}_3)_2]_2$  and  $(\text{Me}_3\text{Si})_3\text{CSH}$  in toluene at ca. 20 °C gave the X-ray characterised, crystalline compound *trans*-[ $\{\text{Ge}[\text{N}(\text{SiMe}_3)_2](\text{CH}_2\text{Ph})(\mu\text{-S})\}_2$ ]. Other four-membered ring chalcogenides [ $\{\text{MR}_2(\mu\text{-E})\}_2$ ] had invariably been obtained from a Group 14 metal (M) precursor: e.g., the X-ray authenticated [ $\{\text{GeBu}'_2(\mu\text{-S})\}_2$ ]<sup>4</sup> and [ $\{\text{SnR}_2(\mu\text{-E})\}_2$ ] (R = Bu' or  $\text{MeCH}_2\text{CMe}_2$ )<sup>5</sup> from the appropriate chloride  $\text{MCl}_2\text{R}_2$  and  $\text{Na}_2\text{E}$ .

Such four-membered ring compound formation has required the use of bulky substituents at M; e.g., the cyclotrimers [ $\{\text{SnR}_2(\mu\text{-E})\}_3$ ] are known for R = Me and E = S, Se or Te as well as for R = Ph and E = S or Te. A heterobichalcogenide compound [ $\{\text{Sn}(\text{C}_6\text{H}_2\text{Pr}^i_3-2,4,6)_2\}_2(\mu\text{-O})(\mu\text{-S})$ ] has been reported.<sup>6</sup>

A feature of the bis[bis(trimethylsilyl)amido]tin(IV) cyclic chalcogenides [ $\{\text{Sn}[\text{N}(\text{SiMe}_3)_2]_2(\mu\text{-E})\}_2$ ] (E = S 1, Se 2 or Te 3) described herein together with their germanium analogues, which differentiates them from the previously reported hydrocarbys [ $\{\text{MR}_2(\mu\text{-E})\}_2$ ] (R = Bu',  $\text{MeCH}_2\text{CMe}_2$  or Ph) is that the  $\text{N}(\text{SiMe}_3)_2$  ligand, unlike R, is a good leaving group; this latter aspect will be exploited in the future.

Selected X-ray molecular structural data on some of these four-membered Group 14 metal(IV) cyclic chalcogenides are shown in Table 1.

## Experimental

**General Procedures.**—These were as described in Part 16,<sup>1</sup> except that NMR spectral data were recorded, unless otherwise stated, at 305 K using a Bruker AMX500 spectrometer.

For the known compounds 1–3,<sup>2</sup> characterisation here was

by microanalysis, m.p. and authentic  $^1\text{H}$  NMR spectra; ultimately X-ray crystallography (see below) was employed.

**Synthesis of [ $\{\text{Sn}[\text{N}(\text{SiMe}_3)_2]_2(\mu\text{-S})\}_2$ ] 1.**—(a) *By reflux.* Sublimed sulfur powder (0.17 g, 5.3 mmol) was added to bis[bis(trimethylsilyl)amido]tin(II) (2.3 g, 5.2 mmol) in thf (tetrahydrofuran) (50 cm<sup>3</sup>). The mixture was refluxed for ca. 8 h. The pale yellow reaction mixture was cooled to room temperature and the small amount of unreacted sulfur and other insolubles were filtered off yielding a yellow filtrate, which was concentrated *in vacuo*. A colourless-to-opaque crystalline solid was obtained, from which the volatiles were removed *in vacuo*. The residual solid was extracted into  $\text{C}_5\text{H}_{12}$  (ca. 30 cm<sup>3</sup>). The extract was concentrated to ca. 10 cm<sup>3</sup> and was stored at –10 °C. After 1 week, colourless crystals of 1 (1.54 g, 63%) were obtained, which were dried slowly *in vacuo*.

(b) *By sonication.* Sublimed sulfur (0.35 g, 11.0 mmol) was added to bis[bis(trimethylsilyl)amido]tin(II) (4.55 g, 10.3 mmol) in thf (ca. 50 cm<sup>3</sup>). The vessel was immersed in an ultrasonic cleaning bath which was preset at 25 °C. An almost instant colour change to a more intense yellow was observed. The reaction mixture was removed from the bath after 1 h of sonication, then filtered free of the very slight precipitate. Volatiles were removed from the filtrate, yielding a crystalline solid which was extracted into  $\text{C}_5\text{H}_{12}$  (ca. 30 cm<sup>3</sup>). Compound 1 (4.49 g, 91%) was obtained using the work-up procedure of (a).

**Synthesis of [ $\{\text{Sn}[\text{N}(\text{SiMe}_3)_2]_2(\mu\text{-Se})\}_2$ ] 2.**—(a) *By reflux.* Selenium powder (0.4 g, 5.1 mmol) was added to a thf solution (ca. 50 cm<sup>3</sup>) of bis[bis(trimethylsilyl)amido]tin(II) (2.22 g, 5.0 mmol). The mixture was refluxed for ca. 14 h becoming dark brown. After cooling to room temperature, the small amount of unreacted selenium and other insolubles were filtered off yielding a red filtrate, which was concentrated *in vacuo* yielding red needles. Volatiles were removed, the residual solid dried *in vacuo* and extracted into  $\text{C}_5\text{H}_{12}$  (ca. 30 cm<sup>3</sup>). The extract was stored at –30 °C for 1 week. Volatiles were removed slowly *in vacuo* to give red needles of 2 (1.73 g, 67%).

(b) *By sonication.* Selenium powder (0.64 g, 8.1 mmol) was added to a thf solution (ca. 50 cm<sup>3</sup>) of bis[bis(trimethylsilyl)amido]tin(II) (3.6 g, 8.1 mmol). The vessel was immersed in

† Subvalent Group 14 Metal Compounds. Part 17.<sup>1</sup>

Supplementary data available: see Instructions for Authors, *J. Chem. Soc., Dalton Trans.*, 1995, Issue 1, pp. xxv–xxx.

**Table 1** Selected bond lengths ( $\text{\AA}$ ) and angles ( $^\circ$ ) for some four membered ring Group 14 metal(IV) chalcogenides, with estimated standard deviations (e.s.d.s) in parentheses\*

	$[\{\text{SnBu}^{\prime}_2(\mu\text{-S})\}_2]^5$	$[\{\text{SnBu}^{\prime}_2(\mu\text{-Se})\}_2]^5$	$[\{\text{SnBu}^{\prime}_2(\mu\text{-Te})\}_2]^5$	$[\{\text{Ge}[\text{N}(\text{SiMe}_3)_2]_2(\mu\text{-Te})\}_2]^2$
$l_1$	2.442(4)	2.553(2)	2.758(1)	2.559(2)
$l_2$	—	—	—	2.596(2)
$l_3$	2.419(4)	2.549(2)	2.754(1)	2.592(2)
$l_4$	—	—	—	2.595(2)
$l_5$	2.19(1)	2.18(2)	2.20(1)	1.867(12)
$l_6$	2.23(1)	2.17(2)	2.21(1)	1.869(10)
$l_7$	—	—	—	1.873(12)
$l_8$	—	—	—	1.858(13)
$a$	93.8(1)	97.5(1)	100.0(1)	94.28(6)
$b$	—	—	—	94.47(6)
$c$	—	—	—	85.59(6)
$d$	86.2(1)	82.5(1)	80.0(1)	85.58(6)
$e$	117.0(6)	115.4(8)	117.0(4)	108.1(5)
$f$	—	—	—	109.0(6)

\* Data shown are for monoclinic crystals.

an ultrasonic cleaning bath preset at 25 °C. The red reaction mixture was removed from the bath after 4 h of sonication, then filtered giving a red filtrate. Using the work-up procedure of (a), red crystals of **2** (2.86 g, 92%) were obtained.

*Synthesis of  $[\{\text{Sn}[\text{N}(\text{SiMe}_3)_2]_2(\mu\text{-Te})\}_2]$  3.*—(a) *By reflux.* Tellurium powder (0.56 g, 4.4 mmol) was added to a thf solution (ca. 50 cm<sup>3</sup>) of bis[bis(trimethylsilyl)amido]tin(II) (1.86 g, 4.2 mmol). The mixture was refluxed for ca. 17 h. The dark brown reaction mixture was allowed to cool to room temperature, and the small amount of unreacted tellurium and other insolubles were filtered off, to give a dark red filtrate. Volatiles were removed from the filtrate *in vacuo* yielding red needles, which were extracted into C<sub>5</sub>H<sub>12</sub> (ca. 30 cm<sup>3</sup>). The resulting red solution was stored at -30 °C for 1 week. Volatiles were very slowly removed *in vacuo* to provide red needles of **3** (1.62 g, 68%) which were dried *in vacuo*.

(b) *By sonication.* Tellurium powder (1.41 g, 11.1 mmol) was added to a thf solution (ca. 50 cm<sup>3</sup>) of bis[bis(trimethylsilyl)amido]tin(II) (4.86 g, 11.0 mmol). The vessel was immersed in an ultrasonic bath preset at 25 °C, and 4 h of sonication was carried out yielding a dark red reaction mixture. Using the work-up procedure of (a), red crystals of **3** (5.75 g, 92%) were obtained.

*Synthesis of  $[(\text{Me}_3\text{Si})_2\text{N}]_2\text{Ge}(\mu\text{-Te})_2\text{Sn}[\text{N}(\text{SiMe}_3)_2]_2$  4.*—Tellurium powder (1.95 g, 15.3 mmol) was added to a thf solution (ca. 50 cm<sup>3</sup>) containing Ge[N(SiMe<sub>3</sub>)<sub>2</sub>]<sup>7</sup> (1.96 g, 5.0 mmol) and Sn[N(SiMe<sub>3</sub>)<sub>2</sub>]<sub>2</sub> (4.47 g, 10 mmol); the mixture was refluxed for ca. 10 h. The cooled, dark brown reaction mixture was filtered through a cannula, yielding a dark red filtrate and a black powder. Red needles were obtained upon removal of volatiles from the filtrate *in vacuo* which were then extracted into C<sub>5</sub>H<sub>12</sub> (ca. 30 cm<sup>3</sup>) to give a red solution. Slowly concentrating the solution *in vacuo* and placing it at -30 °C for 1 week yielded a mixture of mainly orange-red, with a small amount of red, needles. Further removal of volatiles was carried out *in vacuo* and a mixture (2.33 g) of orange-red needles **4** and red needles [ $[\{\text{Ge}[\text{N}(\text{SiMe}_3)_2]_2(\mu\text{-Te})\}_2]$ ] **3** was obtained. The yield of **4** based on the <sup>119</sup>Sn-<sup>1</sup>H NMR spectra of the mixture was 68%. Crystals of compound **4** (0.65 g, 12%), m.p. 145 °C (decomp.) (Found: C, 26.4; H, 6.45; N, 4.95. C<sub>24</sub>H<sub>72</sub>GeN<sub>4</sub>-

Si<sub>8</sub>SnTe<sub>2</sub> requires C, 25.7; H, 6.40; N, 5.00%) were separated manually.

*Reaction of  $[\{\text{Ge}[\text{N}(\text{SiMe}_3)_2]_2(\mu\text{-Te})\}_2]$  and  $[\{\text{Sn}[\text{N}(\text{SiMe}_3)_2]_2(\mu\text{-Te})\}_2]$  with Selenium.*—Selenium powder (1.18 g, 15 mmol) was added to a thf solution (ca. 50 cm<sup>3</sup>) of Ge[N(SiMe<sub>3</sub>)<sub>2</sub>]<sub>2</sub> (1.96 g, 5 mmol) and Sn[N(SiMe<sub>3</sub>)<sub>2</sub>]<sub>2</sub> (2.19 g, 5 mmol); the mixture was refluxed for ca. 12 h. The cooled, dark brown reaction mixture was filtered through a cannula, yielding a dark red filtrate and a very small amount of black precipitate. Volatiles were removed from the filtrate *in vacuo* affording red needles. Pentane (ca. 50 cm<sup>3</sup>) was added and the resulting red mixture was filtered through a cannula, yielding a bright red filtrate, which was concentrated *in vacuo* to ca. 30 cm<sup>3</sup>. Red needles crystallised from the solution after 1 week at -30 °C. After further removal of volatiles, a mixture (2.95 g) of red needles ([ $[\{\text{Ge}[\text{N}(\text{SiMe}_3)_2]_2(\mu\text{-Se})\}_2]$ , [ $[\{\text{Sn}[\text{N}(\text{SiMe}_3)_2]_2(\mu\text{-Se})\}_2]$ ] **2** and [ $[(\text{Me}_3\text{Si})_2\text{N}]_2\text{Ge}(\mu\text{-Se})_2\text{Sn}[\text{N}(\text{SiMe}_3)_2]_2$ ] **5**] was obtained; the evidence for these structural assignments is outlined in the Results and Discussion section.

*X-Ray Data Collection, Structure Solution and Refinement for the Group 14 Metal(IV) Chalcogenides 1–4.*—The appropriate details are in Table 2. Single crystals of each complex were mounted inside a Lindemann capillary and sealed under argon. Cell dimensions were calculated from the setting angles for 25 reflections with  $8 < \theta < 15^\circ$ . Unique data sets were recorded at 173 K for **1**, **2** and **4** or 293 K for **3** on an Enraf-Nonius CAD4 diffractometer. Reflections were corrected for Lorentz and polarization ( $L_p$ ) effects and also for absorption using DIFABS.<sup>8</sup> Intensities were measured by an  $\omega-\theta$  scan and reflections were regarded as observed if  $I > n\sigma(I)$  ( $n = 2$  for **1**, **3** and **4** or  $n = 3$  for **2**). The weighting scheme was  $w = 1/\sigma^2(F)$ , where  $\sigma(F^2) = [\sigma^2(I) + (0.004I)^2]^{1/2}/L_p$ . Structure solution was by routine heavy atom methods. Refinement was by full-matrix least-squares with non-H atoms anisotropic based on  $F$  using programs from the Enraf-Nonius MOLEN package.<sup>9</sup> Hydrogen atoms were fixed either at positions from a difference map or at calculated positions. Further details are in Table 2.

Additional material available from the Cambridge Crystallographic Data Centre comprises H-atom coordinates, thermal parameters and remaining bond lengths and angles.

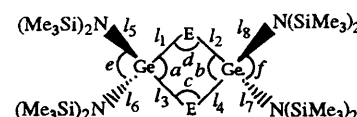
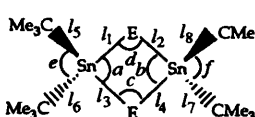
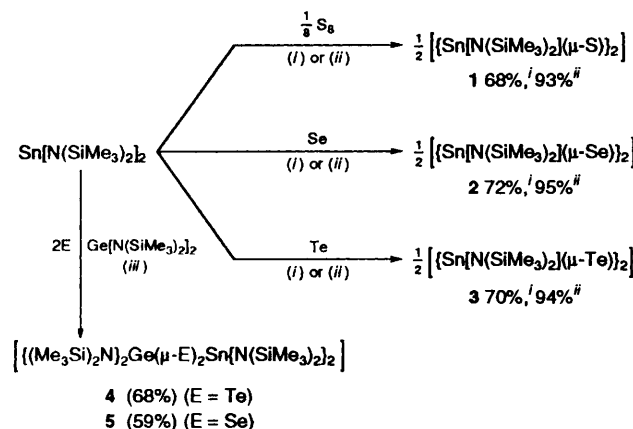


**Table 2** Crystal data for compounds **1–4\***

	<b>1</b>	<b>2</b>	<b>3</b>	<b>4</b>
Formula	$C_{24}H_{72}N_4S_2Si_8Sn_2$	$C_{24}H_{72}N_4Se_2Si_8Sn_2$	$C_{24}H_{72}N_4Si_8Sn_2Te_2$	$C_{24}H_{72}N_4GeSi_8SnTe_2$
<i>M</i>	943.1	1036.9	1134.1	1088.0
Crystal size/mm	0.2 × 0.2 × 0.2	0.25 × 0.25 × 0.25	0.3 × 0.15 × 0.1	0.3 × 0.3 × 0.2
<i>a</i> /Å	9.444(2)	8.905(4)	8.754(2)	8.709(2)
<i>b</i> /Å	11.310(4)	11.291(7)	11.357(1)	11.095(7)
<i>c</i> /Å	23.727(7)	12.925(4)	26.402(3)	26.098(14)
$\alpha/^\circ$	79.49(3)	107.02(4)	79.07(1)	78.52(5)
$\beta/^\circ$	88.12(3)	93.41(3)	81.82(1)	80.55(3)
$\gamma/^\circ$	68.80(3)	109.79(4)	73.24(1)	73.37(4)
<i>U</i> /Å <sup>3</sup>	2321.5	1151.0	2457.2	2352.4
<i>Z</i>	2	1	2	2
<i>D</i> <sub>s</sub> /g cm <sup>-3</sup>	1.35	1.50	1.53	1.54
$\mu/cm^{-1}$	13.9	28.8	24.0	26.03
No. of observed reflections [ $ F^2  > 2\sigma(F^2)$ ]	5027	3652	5462	4688
<i>R</i>	0.085	0.025	0.048	0.040
<i>R'</i>	0.114	0.034	0.065	0.045
<i>A</i> <sub>max,min</sub>	1.09, 0.85	1.09, 0.93	1.04, 0.86	1.07, 0.91
Goodness of fit	2.2	1.2	2.2	2.0
$\Delta\rho_{max,min}/e\text{ Å}^{-3}$	1.8, -2.8	0.6, -0.7	2.5, -1.6	0.9, -0.2

\* Details in common: triclinic, space group *P*ī (no. 2),  $\lambda(\text{Mo-K}\alpha) = 0.71069\text{ \AA}$ .



**Scheme 1** New data on the synthesis of  $[\{\text{Sn}[\text{N}(\text{SiMe}_3)_2]_2(\mu-\text{E})\}]_2$  ( $\text{E} = \text{S} 1, \text{Se} 2$  or  $\text{Te} 3$ ) and the heterobimetallic compounds **4** and **5**: (i) reflux for 8 (**1**), 14 (**2**), or 17 h (**3**) using thf as solvent; (ii) by sonication at 25 °C for 1 (**1**), 4 (**2**) or 4 h (**3**) using thf as solvent; (iii) reflux for 10 h in thf using the ratios: 1Ge, 1Sn, 3Te or 3Se. Yields were derived by integration of the  $\delta^{(119)\text{Sn}}$  signals, using  $^{119}\text{Sn}-\{^1\text{H}\}$  NMR spectroscopy. Crystals were obtained by recrystallisation from  $\text{C}_5\text{H}_{12}$ .

## Results and Discussion

**Synthesis and NMR Spectral Data for  $[\{\text{Sn}[\text{N}(\text{SiMe}_3)_2]_2(\mu-\text{E})\}]_2$  ( $\text{E} = \text{S} 1, \text{Se} 2$  or  $\text{Te} 3$ ) and  $[(\text{Me}_3\text{Si})_2\text{N}_2\text{Ge}(\mu-\text{E})_2\text{Sn}[\text{N}(\text{SiMe}_3)_2]_2]$  ( $\text{E} = \text{Te} 4$  or  $\text{Se} 5$ )**.—Improved yields (*cf.* ref. 2) of each of the compounds **1–3** were obtained by prolonged reflux of  $\text{Sn}[\text{N}(\text{SiMe}_3)_2]_2$  with 2 equivalents of  $\text{E}$  in thf [(i) in Scheme 1]. By use of ultrasound, almost quantitative yields were obtained at ambient temperature in thf after a short reaction time [(ii) in Scheme 1].

By refluxing equimolar portions of  $\text{Sn}[\text{N}(\text{SiMe}_3)_2]_2$  and  $\text{Ge}[\text{N}(\text{SiMe}_3)_2]_2$  with 2 equivalents of  $\text{Te}$  in thf, a mixture of  $[\{\text{Sn}[\text{N}(\text{SiMe}_3)_2]_2(\mu-\text{Te})\}]_2$  (27.6%),  $[\{\text{Ge}[\text{N}(\text{SiMe}_3)_2]_2(\mu-\text{Te})\}]_2$  (18.4%), and compound **4** (54%), based on  $^{125}\text{Te}-\{^1\text{H}\}$  NMR spectra, was obtained. To increase the yield of compound **4**, the stoichiometrically unbalanced reaction of  $\text{Sn}[\text{N}(\text{SiMe}_3)_2]_2$  with  $\text{Ge}[\text{N}(\text{SiMe}_3)_2]_2$  and  $\text{Te}$  in the ratio 2:1:3 was carried out. Based on  $^{125}\text{Te}-\{^1\text{H}\}$  NMR spectra, an improved yield (69%) of **4** was recorded. However from equimolar portions of **2** and **3** and  $\text{Sn}[\text{N}(\text{SiMe}_3)_2]_2:\text{Se}:\text{Te}$  in the ratio 2:1:1 only mixtures of  $[\{\text{Ge}[\text{N}(\text{SiMe}_3)_2]_2(\mu-\text{Te})\}]_2$  and  $[\{\text{Sn}[\text{N}(\text{SiMe}_3)_2]_2(\mu-\text{Te})\}]_2$  **3** were identified.

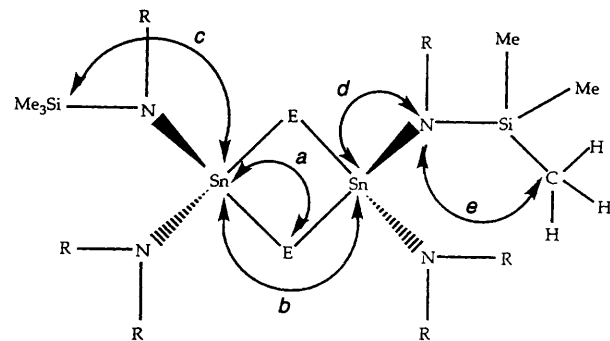


**Fig. 1** Selected NMR spectral coupling information available for  $[\{\text{Sn}[\text{N}(\text{SiMe}_3)_2]_2(\mu-\text{E})\}]_2$  ( $\text{E} = \text{S} 1, \text{Se} 2$  or  $\text{Te} 3$ ): *a*  $^1\text{J}(^{119}\text{Sn}-^{77}\text{Se})$  and  $^1\text{J}(^{117}\text{Sn}-^{77}\text{Se})$  for **2** and  $^1\text{J}(^{119}\text{Sn}-^{125}\text{Te})$  and  $^1\text{J}(^{117}\text{Sn}-^{125}\text{Te})$  for **3**; *b*  $^2\text{J}(^{119}\text{Sn}-^{117}\text{Sn})$ ; *c*  $^2\text{J}(^{119}\text{Sn}-^{29}\text{Si})$ , only obtained for **1**; *d*  $^1\text{J}(^{15}\text{N}-^{119}\text{Sn})$ ; *e*  $^3\text{J}(^{15}\text{N}-^1\text{H})$ .

The new data on compounds **1–5** are summarised in Tables 3 and 4 (not **5**);  $^1\text{H}$  and  $^{13}\text{C}-\{^1\text{H}\}$  NMR spectral chemical shifts for **1–3** were reported previously.<sup>2</sup>

Colourless **1**, red **2** and **3** and orange-red **4** needles were readily obtained by recrystallisation from  $\text{C}_5\text{H}_{12}$ . Precipitation of (chalcogen) powder for each of the compounds **1–4** in  $\text{C}_5\text{H}_{12}$  solution was observed; precipitation of a white **1** or black **2–4** powder was noted after the mixture had been kept at  $-30\text{ }^\circ\text{C}$  under argon for *ca.* 5 d. When any of the compounds **1–4** was kept under argon at room temperature and exposed to light, a faster decomposition rate was found, chalcogen precipitating in *ca.* 2 d.

In addition to the fact that compounds **1–5** have numerous NMR-active spin  $\frac{1}{2}$  nuclei, most of them are located next to one another. Hence central ring structures were deduced by determining one-bond coupling constants between chalcogen ( $^{77}\text{Se}$  or  $^{125}\text{Te}$ ) and tin ( $^{117}\text{Sn}$  and  $^{119}\text{Sn}$ ), and also the transannular  $^{119}\text{Sn}-^{117}\text{Sn}$  coupling constant for each of the compounds **1–3**. From chemical shifts and coupling constants based on the  $^1\text{H}$ ,  $^{13}\text{C}$ ,  $^{15}\text{N}$  and  $^{29}\text{Si}$  nuclei, it was established that the two  $\text{N}(\text{SiMe}_3)_2$  ligands at Sn remained intact. Fig. 1 shows this ‘NMR-friendly’ environment for compounds **1–3**; parameters *a* and *c–e* (Fig. 1) are also relevant to compounds **4** and **5**. The  $^{119}\text{Sn}-\{^1\text{H}\}$  spectrum of compounds **1–3** revealed a single signal flanked by one set of satellites, assigned to

**Table 3** Summary of new characterising (excluding detailed X-ray) data obtained for  $\left[\{\text{Sn}(\text{SiMe}_3)_2\}_2(\mu\text{-E})_2\right]$  ( $\text{E} = \text{S} 1$ ,  $\text{Se} 2$  or  $\text{Te} 3$ ) and  $\left[\{(\text{Me}_3\text{Si})_2\text{N}\}_2\text{Ge}(\mu\text{-E})_2\text{Sn}\{\text{N}(\text{SiMe}_3)_2\}_2\right]$  ( $\text{E} = \text{Te} 4$  or  $\text{Se} 5$ )

Proton-decoupled NMR spectral data <sup>a</sup>						
Compound	Crystal appearance	Yield (%)	$^{29}\text{Si}\{-^1\text{H}\}$	$^{77}\text{Se}\{-^1\text{H}\}$	$^{119}\text{Sn}\{-^1\text{H}\}$	$^{125}\text{Te}\{-^1\text{H}\}$
<b>1</b>	Colourless needles, triclinic	63, <sup>b</sup> 91 <sup>c</sup>	+7.4, $^{2}J(^{29}\text{Si}-^{119}\text{Sn})$	—	-106.6, $^{2}J(^{119}\text{Sn}-^{117}\text{Sn}) = 609$	—
			= 13			
<b>2</b>	Red needles, triclinic	67, <sup>b</sup> 92 <sup>c</sup>	+ 7.3	- 640.1, $^{1}J(^{77}\text{Se}-^{119}\text{Sn}) = 1129$ , $^{1}J(^{77}\text{Se}-^{117}\text{Sn}) = 1028$	- 382.6, $^{1}J(^{119}\text{Sn}-^{77}\text{Se}) = 1129$ , $^{2}J(^{119}\text{Sn}-^{117}\text{Sn}) = 786$	- 322.2, $^{1}J(^{119}\text{Sn}-^{119}\text{Sn}) = 5$
<b>3</b>	Red needles, triclinic	68, <sup>b</sup> 92 <sup>c</sup>	+ 7.3	—	- 988.8, $^{1}J(^{119}\text{Sn}-^{125}\text{Te}) =$ $2711, ^{2}J(^{119}\text{Sn}-^{117}\text{Sn}) = 567$	- 326.7, $^{1}J(^{119}\text{Sn}-^{119}\text{Sn}) = 5$
<b>4<sup>d</sup></b>	Orange-red needles, triclinic	68 <sup>e</sup>	+ 5.47 (Ge), + 8.13 (Sn)	—	- 1023.9, $^{1}J(^{119}\text{Sn}-^{125}\text{Te}) =$ $2778$	- 317.1 (Ge), - 332.1 (Sn), $^{1}J(^{119}\text{Sn}-^{119}\text{Sn}) = 5$
<b>5</b>	Not isolated as pure material	59 <sup>e,f</sup>	+ 5.41 (Ge), + 8.13 (Sn)	- 565.2 + 8.13 (Sn)	- 422.6, $^{1}J(^{119}\text{Sn}-^{77}\text{Se}) =$ 1111.1	- 313.2 (Ge), - 332.1 (Sn)

<sup>a</sup>The multinuclear NMR spectra were recorded at 305 K in C<sub>6</sub>D<sub>6</sub> on a Bruker AMX500 spectrometer; chemical shifts ( $\delta$ ) are relative to those for SiMe<sub>4</sub> (<sup>29</sup>Si), SeMe<sub>2</sub> (<sup>77</sup>Se), SnMe<sub>2</sub> (<sup>119</sup>Sn), TeMe<sub>2</sub> (<sup>125</sup>Te) and MeNO<sub>2</sub> (<sup>15</sup>N) coupling constants are in Hz. <sup>b</sup> Isolated yield obtained by method (i) of Scheme 1. <sup>c</sup> Isolated yield obtained by method (ii) of Scheme 1. <sup>d</sup>  $\delta(^1\text{H}) = +0.48$ ,  $\delta(^{13}\text{C}\{-^1\text{H}\}) = +7.3$ . <sup>e</sup> Yield based on integral of <sup>119</sup>Sn-<sup>{1}H</sup> NMR spectral signals. <sup>f</sup> Yield also based on integral of <sup>77</sup>Se-<sup>{1}H</sup> spectral signals.

**Table 4** Multinuclear NMR spectroscopic data<sup>a</sup> for Ge[N(SiMe<sub>3</sub>)<sub>2</sub>]<sub>2</sub> and [{Ge[N(SiMe<sub>3</sub>)<sub>2</sub>]<sub>2</sub>(μ-E)}<sub>2</sub>] (E = Se or Te)

Compound	δ( <sup>1</sup> H)	δ( <sup>13</sup> C-{ <sup>1</sup> H})	δ(INEPT <sup>15</sup> N)	δ( <sup>29</sup> Si-{ <sup>1</sup> H})	δ(E-{ <sup>1</sup> H})
Ge[N(SiMe <sub>3</sub> ) <sub>2</sub> ] <sub>2</sub>	0.49 <sup>b</sup>	7.33	-320.4	5.45	—
[{Ge[N(SiMe <sub>3</sub> ) <sub>2</sub> ] <sub>2</sub> (μ-Se)} <sub>2</sub> ]	0.50	7.21 <sup>c</sup>	-318.5	5.81	-476.0
[{Ge[N(SiMe <sub>3</sub> ) <sub>2</sub> ] <sub>2</sub> (μ-Te)} <sub>2</sub> ]	0.48	7.30 <sup>d</sup>	-320.3	5.47	1184

<sup>a</sup> All NMR spectra were obtained in C<sub>6</sub>D<sub>6</sub> at ambient temperature on a Bruker AMX500 instrument. <sup>b</sup> cf. δ(<sup>1</sup>H) 0.44, ref. 7. <sup>c</sup> cf. δ(<sup>13</sup>C) 7.29, ref. 2. <sup>d</sup> cf. δ(<sup>13</sup>C) 7.53, ref. 2.

**Table 5** Intramolecular distances (Å) and angles (°) for [{Sn[N(SiMe<sub>3</sub>)<sub>2</sub>]<sub>2</sub>(μ-S)}<sub>2</sub>] 1 with e.s.d.s in parentheses

Sn(1)-S(1)	2.416(5)	Sn(1)-S(2)	2.413(6)
Sn(1)-N(1)	2.034(13)	Sn(1)-N(2)	2.08(2)
Sn(2)-S(1)	2.427(6)	Sn(2)-S(2)	2.409(5)
Sn(2)-N(3)	2.061(12)	Sn(2)-N(4)	2.07(2)
Si(1)-N(1)	1.74(5)	Si(1)-C(1)	1.94(6)
Si(1)-C(2)	1.86(3)	Si(1)-C(3)	1.86(3)
Si(2)-N(1)	1.78(2)	Si(2)-C(4)	1.85(2)
Si(2)-C(5)	1.86(2)	Si(2)-C(6)	1.95(2)
Si(3)-N(2)	1.74(2)	Si(3)-C(7)	1.95(2)
Si(3)-C(8)	1.82(2)	Si(3)-C(9)	1.85(2)
Si(4)-N(2)	1.72(2)	Si(4)-C(10)	1.86(2)
Si(4)-C(11)	1.84(2)	Si(4)-C(12)	1.86(2)
Si(5)-N(3)	1.76(2)	Si(5)-C(13)	1.86(2)
Si(5)-C(14)	1.88(3)	Si(5)-C(15)	1.87(2)
Si(6)-N(3)	1.74(2)	Si(6)-C(16)	1.88(2)
Si(6)-C(17)	1.86(3)	Si(6)-C(18)	1.87(2)
Si(7)-N(4)	1.70(2)	Si(7)-C(19)	1.87(2)
Si(7)-C(20)	1.83(2)	Si(7)-C(21)	1.88(2)
Si(8)-N(4)	1.78(2)	Si(8)-C(22)	1.84(2)
Si(8)-C(23)	1.94(2)	Si(8)-C(24)	1.89(3)
S(1)-Sn(1)-S(2)	93.5(2)	S(1)-Sn(1)-N(1)	110.9(5)
S(1)-Sn(1)-N(2)	115.1(4)	S(2)-Sn(1)-N(1)	114.8(5)
S(2)-Sn(1)-N(2)	108.6(5)	N(1)-Sn(1)-N(2)	112.7(6)
S(1)-Sn(2)-S(2)	93.3(2)	S(1)-Sn(2)-N(3)	114.6(5)
S(1)-Sn(2)-N(4)	108.2(4)	S(2)-Sn(2)-N(3)	109.2(4)
S(2)-Sn(2)-N(4)	115.3(4)	N(3)-Sn(2)-N(4)	114.6(6)
Sn(1)-Si(1)-Sn(2)	86.4(2)	Sn(1)-S(2)-Sn(2)	86.9(2)
N(1)-Si(1)-C(1)	113(1)	S(1)-Si(1)-C(2)	109(1)
N(1)-Si(1)-C(3)	111(1)	C(1)-Si(1)-C(2)	113(1)
C(1)-Si(1)-C(3)	101(1)	C(2)-Si(1)-C(3)	110(2)
N(1)-Si(2)-C(4)	111(1)	N(1)-Si(2)-C(5)	112(1)
N(1)-Si(2)-C(6)	111.8(9)	C(4)-Si(2)-C(5)	106(1)
C(4)-Si(2)-C(6)	112(1)	C(5)-Si(2)-C(6)	104(1)
N(2)-Si(3)-C(7)	113.8(8)	N(2)-Si(3)-C(8)	110.8(9)
N(2)-Si(3)-C(9)	111(1)	C(7)-Si(3)-C(8)	105(1)
C(7)-Si(3)-C(9)	109(1)	C(8)-Si(3)-C(9)	107(1)
N(2)-Si(4)-C(10)	111(1)	N(2)-Si(4)-C(11)	109.5(9)
N(2)-Si(4)-C(12)	111(1)	C(10)-Si(4)-C(11)	111(1)
C(10)-Si(4)-C(12)	106(1)	C(11)-Si(4)-C(12)	108(1)
C(22)-Si(8)-C(24)	106(1)	C(23)-Si(8)-C(24)	108(1)
Sn(1)-N(1)-Si(1)	117.9(9)	Sn(1)-N(1)-Si(2)	119(1)
Si(1)-N(1)-Si(2)	121.0(8)	Sn(1)-N(2)-Si(3)	119.3(8)
Sn(1)-N(2)-Si(4)	114.3(9)	Si(3)-N(2)-Si(4)	122.6(9)
Sn(2)-N(3)-Si(5)	124.0(8)	Sn(2)-N(3)-Si(6)	117.3(8)
Si(5)-N(3)-Si(6)	118.7(7)	Sn(2)-N(4)-Si(7)	117.5(9)
Sn(2)-N(4)-Si(8)	123.4(8)	Si(7)-N(4)-Si(8)	119.0(9)

<sup>2</sup>J(<sup>119</sup>Sn-<sup>117</sup>Sn). The former had twice the intensity of the latter, consistent with each tin nucleus being coupled to two equivalent selenium nuclei. Comparable conclusions are drawn from the <sup>119</sup>Sn-{<sup>1</sup>H} spectrum of the tellurium compound 3. Each of the <sup>77</sup>Se-{<sup>1</sup>H} (for 2 and 5) and <sup>125</sup>Te-{<sup>1</sup>H} NMR spectra (for 3 and 4) showed a single peak with closely-spaced pairs of satellites due to both <sup>119</sup>Sn and <sup>117</sup>Sn nuclei. Initially (prior to the X-ray analysis) the structure of [{(Me<sub>3</sub>Si)<sub>2</sub>}<sub>2</sub>Ge(μ-Te)Sn{N(SiMe<sub>3</sub>)<sub>2</sub>}<sub>2</sub>] 4 was deduced from the rich NMR spectral information; data and assignments for the selenium analogue 5 are also shown in Table 3.

The insensitive nuclei enhanced by polarization transfer

**Table 6** Selected intramolecular distances (Å) and angles (°) for [{Sn[N(SiMe<sub>3</sub>)<sub>2</sub>]<sub>2</sub>(μ-Se)}<sub>2</sub>] 2

Sn-Se	2.544(1)	Sn-Se'	2.538(1)
Sn-N(1)	2.050(3)	Sn-N(2)	2.047(2)
Si(1)-N(1)	1.752(2)	Si(1)-C(1)	1.866(4)
Si(1)-C(2)	1.870(4)	Si(1)-C(3)	1.880(5)
Si(2)-N(1)	1.745(3)	Si(2)-C(4)	1.866(4)
Si(2)-N(5)	1.864(4)	Si(2)-C(6)	1.857(5)
Si(3)-N(2)	1.761(3)	Si(3)-C(7)	1.878(3)
Si(3)-C(8)	1.867(4)	Si(3)-C(9)	1.857(5)
Si(4)-N(2)	1.753(2)	Si(4)-C(10)	1.869(5)
Si(4)-C(1)	1.867(4)	Si(4)-C(12)	1.876(4)
Se-Sn-Se'	94.91(1)	Se-Sn-N(1)	115.44(6)
Se-Sn-N(2)	108.74(8)	Se'-Sn-N(1)	109.46(7)
Se'-Sn-N(2)	117.70(7)	N(1)-Sn-N(2)	110.1(1)
Sn-Se-Sn'	85.09(1)	N(1)-Si(1)-C(1)	113.4(2)
N(1)-Si(1)-C(2)	109.4(2)	N(1)-Si(1)-C(3)	112.2(1)
C(1)-Si(1)-C(2)	110.1(2)	C(1)-Si(1)-C(3)	102.9(2)
C(2)-Si(1)-C(3)	108.7(2)	N(1)-Si(2)-C(4)	110.7(2)
N(1)-Si(2)-C(5)	109.3(2)	N(1)-Si(2)-C(6)	115.0(1)
C(4)-Si(2)-C(5)	110.1(2)	C(4)-Si(2)-C(6)	108.0(2)
C(5)-Si(2)-C(6)	103.5(2)	N(2)-Si(3)-C(7)	111.6(1)
N(2)-Si(3)-C(8)	110.3(2)	N(2)-Si(3)-C(9)	111.9(2)
C(7)-Si(3)-C(8)	106.1(2)	C(7)-Si(3)-C(9)	109.3(2)
C(8)-Si(3)-C(9)	107.4(2)	N(2)-Si(4)-C(10)	110.5(2)
N(2)-Si(4)-C(11)	115.0(1)	N(2)-Si(4)-C(12)	111.1(2)
C(10)-Si(4)-C(11)	105.3(2)	C(10)-Si(4)-C(12)	107.4(2)
C(11)-Si(4)-C(12)	107.1(2)	Sn-N(1)-Si(1)	120.1(1)
Sn-N(2)-Si(3)	114.2(1)	Si(1)-N(1)-Si(2)	124.4(2)
Sn-N(2)-Si(3)	113.9(1)	Sn-N(2)-Si(4)	127.7(1)
Si(3)-N(2)-Si(4)	117.9(1)		

Symmetry element ' is -x, -y, -z.

(INEPT) technique was used to obtain <sup>15</sup>N NMR spectral parameters for compounds 1–5. Polarization transfer was from the trimethylsilyl protons via a three-bond N-H coupling, <sup>3</sup>J(<sup>1</sup>H-<sup>15</sup>N). In order to obtain the transfer, the delays within the INEPT pulse had to be lengthened for signal through relaxation. Interestingly, <sup>1</sup>J(<sup>15</sup>N-<sup>119</sup>Sn) for compound 1 was substantial, 28.4 Hz, but for compounds 2–5 the values were small, 5 Hz. The observed <sup>1</sup>H and <sup>13</sup>C-{<sup>1</sup>H} NMR spectral data for 1–3 were consistent with those of earlier work.<sup>2</sup> For compound 4, these were δ(<sup>1</sup>H) 0.48 and δ(<sup>13</sup>C-{<sup>1</sup>H}) 7.3, and similar values were obtained for 5. In order to facilitate the NMR spectral analysis, specimens of Ge[N(SiMe<sub>3</sub>)<sub>2</sub>]<sub>2</sub><sup>7</sup> and [{Ge[N(SiMe<sub>3</sub>)<sub>2</sub>]<sub>2</sub>(μ-E)}<sub>2</sub>] (E = Se or Te)<sup>2</sup> were prepared and multinuclear (<sup>1</sup>H, <sup>13</sup>C, <sup>15</sup>N, <sup>29</sup>Si, <sup>77</sup>Se, <sup>125</sup>Te) NMR spectra were obtained, Table 4. Significant NMR spectral data for Sn[N(SiMe<sub>3</sub>)<sub>2</sub>]<sub>2</sub> including <sup>15</sup>N parameters have been published,<sup>10</sup> as well as its crystal structure.<sup>11</sup>

Attempts to prepare the four-membered ring analogue 5 of compound 4 with selenium in place of Te were also carried out by refluxing Ge[N(SiMe<sub>3</sub>)<sub>2</sub>]<sub>2</sub> with Sn[N(SiMe<sub>3</sub>)<sub>2</sub>]<sub>2</sub> and Se (1:1:3) in thf. A mixture of [{(Me<sub>3</sub>Si)<sub>2</sub>N}<sub>2</sub>Ge(μ-Se)<sub>2</sub>Sn{N(SiMe<sub>3</sub>)<sub>2</sub>}<sub>2</sub>] 5 (59%), [{Ge[N(SiMe<sub>3</sub>)<sub>2</sub>]<sub>2</sub>(μ-Se)}<sub>2</sub>] (12%) and [{Sn[N(SiMe<sub>3</sub>)<sub>2</sub>]<sub>2</sub>(μ-Se)}<sub>2</sub>] 2 (29%) was obtained, the yields being based on <sup>77</sup>Se-{<sup>1</sup>H} and <sup>119</sup>Sn-{<sup>1</sup>H} NMR spectra. Other multinuclear NMR spectra (including <sup>1</sup>H, <sup>13</sup>C-{<sup>1</sup>H}, INEPT

**Table 7** Selected intramolecular distances ( $\text{\AA}$ ) and angles ( $^\circ$ ) for  $[\{\text{Sn}[\text{N}(\text{SiMe}_3)_2]_2(\mu\text{-Te})\}_2]$  3 with e.s.d.s in parentheses

Te(1)–Sn(1)	2.752(1)	Te(1)–Sn(2)	2.757(1)
Te(2)–Sn(1)	2.751(1)	Te(2)–Sn(2)	2.755(1)
Sn(1)–N(1)	2.066(6)	Sn(1)–N(2)	2.062(7)
Sn(2)–N(3)	2.054(8)	Sn(2)–N(4)	2.060(7)
Si(1)–N(1)	1.752(7)	Si(1)–C(1)	1.833(15)
Si(1)–C(2)	1.857(14)	Si(1)–C(3)	1.910(14)
Si(2)–N(1)	1.729(8)	Si(2)–C(4)	1.851(10)
Si(2)–C(5)	1.88(2)	Si(2)–C(6)	1.857(14)
Si(3)–N(2)	1.742(8)	Si(3)–C(7)	1.865(10)
Si(3)–C(8)	1.848(11)	Si(3)–C(9)	1.874(12)
Si(4)–N(2)	1.755(6)	Si(4)–C(10)	1.870(13)
Si(4)–C(11)	1.844(13)	Si(4)–C(12)	1.875(11)
Si(5)–N(3)	1.738(8)	Si(5)–C(13)	1.883(14)
Si(5)–C(14)	1.882(14)	Si(5)–C(15)	1.906(14)
Si(6)–N(3)	1.754(10)	Si(6)–C(16)	1.851(13)
Si(6)–C(17)	2.18(2)	Si(6)–C(18)	1.82(2)
Si(7)–N(4)	1.715(8)	Si(7)–C(19)	1.898(13)
Si(7)–C(20)	1.89(2)	Si(7)–C(21)	1.857(15)
Si(8)–N(4)	1.771(10)	Si(8)–C(22)	1.924(11)
Si(8)–C(23)	1.835(13)	Si(8)–C(24)	1.93(2)
Sn(1)–Te(1)–Sn(2)	83.71(3)	Sn(1)–Te(2)–Sn(2)	83.74(3)
Te(1)–Sn(1)–Te(2)	96.34(3)	Te(1)–Sn(1)–N(1)	106.9(2)
Te(1)–Sn(1)–N(2)	118.7(2)	Te(2)–Sn(1)–N(1)	118.9(2)
Te(2)–Sn(1)–N(2)	107.0(2)	N(1)–Sn(1)–N(2)	109.2(3)
Te(1)–Sn(2)–Te(2)	96.12(3)	Te(1)–Sn(2)–N(3)	109.1(2)
Te(1)–Sn(2)–N(4)	117.5(2)	Te(2)–Sn(2)–N(3)	118.1(2)
Te(2)–Sn(2)–N(4)	108.4(3)	N(3)–Sn(2)–N(4)	107.7(3)
N(1)–Si(1)–C(1)	114.7(5)	N(1)–Si(1)–C(2)	109.8(5)
N(1)–Si(1)–C(3)	110.4(5)	C(1)–Si(1)–C(2)	108.4(7)
C(1)–Si(1)–C(3)	104.9(7)	C(2)–Si(1)–C(3)	108.5(7)
N(1)–Si(2)–C(4)	112.2(4)	N(1)–Si(2)–C(5)	115.5(5)
N(1)–Si(2)–C(6)	110.7(6)	C(4)–Si(2)–C(5)	105.6(6)
C(4)–Si(2)–C(6)	107.6(6)	C(5)–Si(2)–C(6)	109.0(7)
N(2)–Si(3)–C(7)	112.0(4)	N(2)–Si(3)–C(8)	110.2(5)
N(2)–Si(3)–C(9)	112.2(4)	C(7)–Si(3)–C(8)	106.7(5)
C(7)–Si(3)–C(9)	105.8(5)	C(8)–Si(3)–C(9)	109.7(6)
N(2)–Si(4)–C(10)	111.3(5)	N(2)–Si(4)–C(11)	114.3(4)
N(2)–Si(4)–C(12)	110.0(4)	C(10)–Si(4)–C(11)	103.6(6)
C(10)–Si(4)–C(12)	107.7(5)	C(11)–Si(4)–C(12)	109.6(5)
N(3)–Si(5)–C(13)	115.2(5)	N(3)–Si(5)–C(14)	111.4(6)
N(3)–Si(5)–C(15)	109.8(5)	C(13)–Si(5)–C(14)	105.8(6)
C(13)–Si(5)–C(15)	104.1(7)	C(14)–Si(5)–C(15)	110.3(7)
N(3)–Si(6)–C(16)	112.1(5)	N(3)–Si(6)–C(17)	102.9(8)

$^{15}\text{N}$  and  $^{29}\text{Si}-\{\text{H}\}$ ) were consistent with this assignment, Table 3. Attempts to isolate and characterize pure compound 5 failed.

A linear relationship was found between (i) the tin chemical shifts for compounds 1–3 and the Pauling electronegativity of the appropriate chalcogen; (ii)  $\delta(^{125}\text{Te}-\{\text{H}\})$  and  $\chi$  (the Pauling electronegativity) of Ge and Sn for 3, 4 and  $[\{\text{Ge}[\text{N}(\text{SiMe}_3)_2]_2(\mu\text{-Te})\}_2]$ ; and (iii)  $\delta(^{77}\text{Se}-\{\text{H}\})$  and  $\chi$  of Sn and Ge for 5 and 2 and  $[\{\text{Ge}[\text{N}(\text{SiMe}_3)_2]_2(\mu\text{-Se})\}_2]$ .<sup>9</sup>

*Crystal Structures of  $[\{\text{Sn}[\text{N}(\text{SiMe}_3)_2]_2(\mu\text{-E})\}_2]$  (E = S 1, Se 2 or Te 3) and  $[(\text{Me}_3\text{Si})_2\text{N}]_2\text{Ge}(\mu\text{-Te})_2\text{Sn}[\text{N}(\text{SiMe}_3)_2]_2$  4.*—For each of the compounds 1–4, X-ray quality single crystals were obtained from  $\text{C}_5\text{H}_{12}$  solution. Non-hydrogen atom bond lengths and angles are shown in Tables 5–12, and corresponding atomic coordinates in Tables 9–12, respectively. The more significant geometrical parameters, summarised in Fig. 2, may be compared with some literature data shown in Table 1. Fig. 3 illustrates the molecular structure and the atom labelling scheme for each of the compounds 1–4.

In 2 the four-membered ring core of alternating tin and chalcogen atoms is planar by symmetry whilst for the other structures the maximum deviation from planarity of the central ring atoms is 0.006, 0.026 and 0.034  $\text{\AA}$  for 1, 3 and 4, respectively.

**Table 8** Intramolecular distances ( $\text{\AA}$ ) and angles ( $^\circ$ ) for  $[(\text{Me}_3\text{Si})_2\text{N}]_2\text{Ge}(\mu\text{-Te})_2\text{Sn}[\text{N}(\text{SiMe}_3)_2]_2$  4 with e.s.d.s in parentheses

Te(1)–Sn	2.728(1)	Te(1)–Ge	2.615(1)
Te(2)–Sn	2.721(1)	Te(2)–Ge	2.621(1)
Sn–N(3)	2.042(6)	Sn–N(4)	2.032(7)
Ge–N(1)	1.873(7)	Ge–N(2)	1.872(6)
Si(1)–N(1)	1.771(6)	Si(1)–C(1)	1.847(11)
Si(1)–C(2)	1.853(9)	Si(1)–C(3)	1.856(10)
Si(2)–N(1)	1.759(8)	Si(2)–C(4)	1.873(11)
Si(2)–C(5)	1.860(10)	Si(2)–C(6)	1.852(8)
Si(3)–N(2)	1.769(6)	Si(3)–C(7)	1.862(10)
Si(3)–C(8)	1.831(11)	Si(3)–C(9)	1.836(11)
Si(4)–N(2)	1.757(7)	Si(4)–C(10)	1.859(8)
Si(4)–C(11)	1.867(10)	Si(4)–C(12)	1.857(12)
Si(5)–N(3)	1.743(7)	Si(5)–C(13)	1.866(11)
Si(5)–C(14)	1.868(11)	Si(5)–C(15)	1.845(10)
Si(6)–N(3)	1.759(8)	Si(6)–C(16)	1.867(9)
Si(6)–C(17)	1.843(10)	Si(6)–C(18)	1.873(12)
Si(7)–N(4)	1.754(8)	Si(7)–C(19)	1.843(12)
Si(7)–C(20)	1.883(11)	Si(7)–C(21)	1.861(10)
Si(8)–N(4)	1.752(6)	Si(8)–C(22)	1.861(12)
Si(8)–C(23)	1.861(11)	Si(8)–C(24)	1.875(10)
Sn–Te(1)–Ge	84.26(3)	Sn–Te(2)–Ge	84.28(3)
Te(1)–Sn–Te(2)	93.14(3)	Te(1)–Sn–N(3)	108.8(2)
Te(1)–Sn–N(4)	118.8(2)	Te(2)–Sn–N(3)	118.1(2)
Te(2)–Sn–N(4)	110.9(2)	N(3)–Sn–N(4)	107.1(3)
Te(1)–Ge–Te(2)	98.18(3)	Te(1)–Ge–N(1)	107.2(2)
Te(1)–Ge–N(2)	117.1(2)	Te(2)–Ge–N(1)	118.0(2)
Te(2)–Ge–N(2)	107.6(2)	N(1)–Ge–N(2)	109.0(3)
N(1)–Si(1)–C(1)	115.8(4)	N(1)–Si(1)–C(2)	109.5(4)
N(1)–Si(1)–C(3)	111.1(4)	C(1)–Si(1)–C(2)	110.0(4)
C(1)–Si(1)–C(3)	101.9(5)	C(2)–Si(1)–C(3)	108.1(4)
N(1)–Si(2)–C(4)	111.7(4)	N(1)–Si(2)–C(5)	110.7(4)
N(1)–Si(2)–C(6)	112.2(4)	C(4)–Si(2)–C(5)	110.4(5)
C(4)–Si(2)–C(6)	105.2(4)	C(5)–Si(2)–C(6)	106.4(4)
N(2)–Si(3)–C(7)	111.9(4)	N(2)–Si(3)–C(8)	110.0(4)
N(2)–Si(3)–C(9)	115.6(4)	C(7)–Si(3)–C(8)	108.6(5)
C(7)–Si(3)–C(9)	102.2(5)	C(8)–Si(3)–C(9)	108.2(5)
N(2)–Si(4)–C(10)	112.0(4)	N(2)–Si(4)–C(11)	111.1(4)
N(2)–Si(4)–C(12)	111.7(4)	C(10)–Si(4)–C(11)	106.1(4)
C(10)–Si(4)–C(12)	105.0(5)	C(11)–Si(4)–C(12)	110.6(5)
N(3)–Si(5)–C(13)	111.1(4)	N(3)–Si(5)–C(14)	111.3(5)
N(3)–Si(5)–C(15)	115.8(4)	C(13)–Si(5)–C(14)	107.2(5)
C(13)–Si(5)–C(15)	106.8(5)	C(14)–Si(5)–C(15)	103.9(5)
N(3)–Si(6)–C(16)	111.2(4)	N(3)–Si(6)–C(17)	112.7(5)
N(3)–Si(6)–C(18)	112.3(4)	C(16)–Si(6)–C(17)	105.1(4)
C(16)–Si(6)–C(18)	107.5(5)	C(17)–Si(6)–C(18)	107.6(5)
N(4)–Si(7)–C(19)	113.6(4)	N(4)–Si(7)–C(20)	111.6(5)
N(4)–Si(7)–C(21)	109.8(4)	C(19)–Si(7)–C(20)	107.4(5)
C(19)–Si(7)–C(21)	104.1(5)	C(20)–Si(7)–C(21)	110.0(4)
N(4)–Si(8)–C(22)	115.6(4)	N(4)–Si(8)–C(23)	110.9(4)
N(4)–Si(8)–C(24)	109.8(4)	N(22)–Si(8)–C(23)	106.9(5)
C(22)–Si(8)–C(24)	104.8(5)	C(23)–Si(8)–C(24)	108.5(5)
Ge–N(1)–Si(1)	120.9(4)	Ge–N(1)–Si(2)	117.4(3)
Si(1)–N(1)–Si(2)	117.6(4)	Ge–N(2)–Si(3)	120.9(4)
Ge–N(2)–Si(4)	117.6(3)	Si(3)–N(2)–Si(4)	117.2(4)
Sn–N–Si(5)	128.3(4)	Sn–N(3)–Si(6)	113.2(3)
Si(5)–N(3)–Si(6)	117.8(4)	Sn–N(4)–Si(7)	114.7(3)
Sn–N(4)–Si(8)	126.7(4)	Si(7)–N(4)–Si(8)	118.6(4)

Two bulky  $\text{N}(\text{SiMe}_3)_2$  groups are attached to each tin atom (also Ge for 4) with one above and the other below the ring plane. Compounds 1 and 3 show slightly distorted ring planes, while compound 2 has an inversion centre at the mid-point of the ring; 4 also has a planar ring core. Bond lengths between tin and chalcogen increase with atomic number of E. The Sn–N bond lengths for compounds 1–4 are reduced by *ca.* 0.02–0.06  $\text{\AA}$ , and the N–Sn–N angles are increased by *ca.* 2.5–9.9°, compared with the values for the tin(II) starting material  $\text{Sn}[\text{N}(\text{SiMe}_3)_2]_2$ , [Sn–N 2.096(1) and 2.088(6)  $\text{\AA}$ , and N–Sn–N 104.7(2)°].<sup>11</sup> This is attributed mainly to the radius of  $\text{Sn}^{4+}$

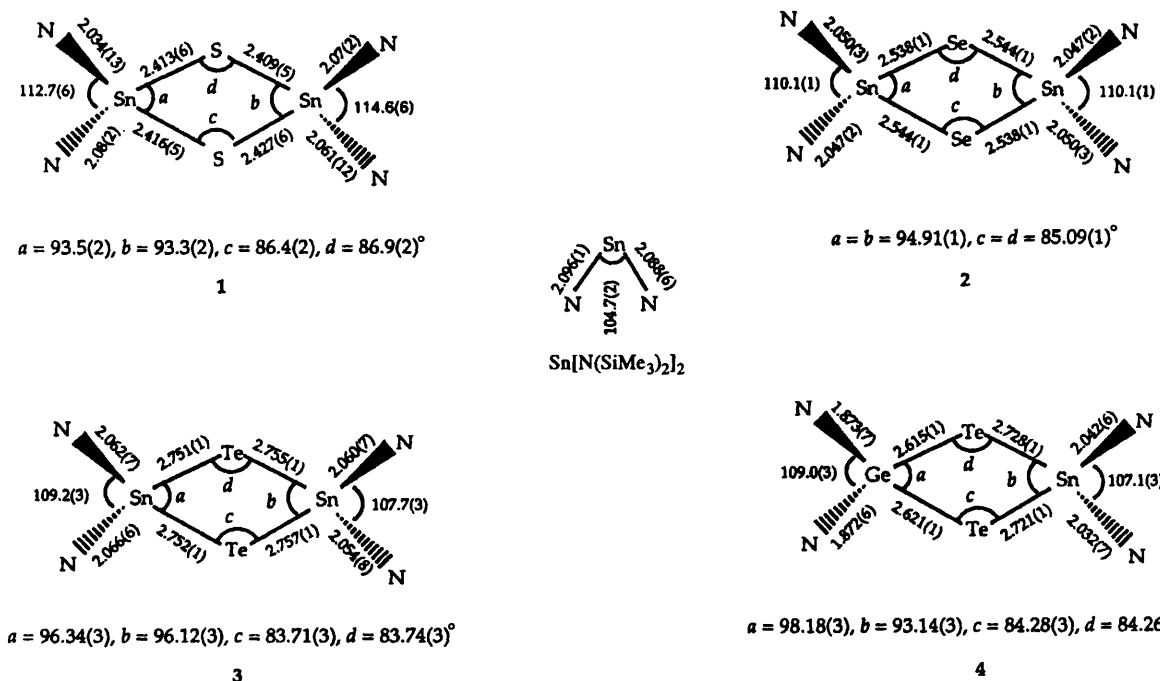


Fig. 2 Selected bond lengths ( $\text{\AA}$ ) and angles ( $^\circ$ ) for  $[\{\text{Sn}[\text{N}(\text{SiMe}_3)_2]_2(\mu\text{-E})\}_2]$  ( $\text{E} = \text{S}$  1,  $\text{Se}$  2 or  $\text{Te}$  3),  $[(\text{Me}_3\text{Si})_2\text{N}]_2\text{Ge}(\mu\text{-Te})_2\text{Sn}[\text{N}(\text{SiMe}_3)_2]_2$  4 and  $\text{Sn}[\text{N}(\text{SiMe}_3)_2]_2^{11}$  with e.s.d.s in parentheses

Table 9 Fractional atomic coordinates ( $\times 10^4$ ) for compound 1

Atom	<i>x</i>	<i>y</i>	<i>z</i>
Sn(1)	557.0(14)	2012.8(12)	1809.6(6)
Sn(2)	1959.7(13)	1638.7(11)	3120.3(5)
S(1)	-110(5)	1175(4)	2750(2)
S(2)	2595(5)	2493(4)	2181(2)
Si(1)	-2736(7)	3325(6)	1147(3)
Si(2)	-1371(7)	5136(5)	1534(3)
Si(3)	1923(6)	-974(5)	1570(2)
Si(4)	2302(7)	1179(5)	685(2)
Si(5)	3614(6)	-1417(5)	3840(3)
Si(6)	5579(6)	99(5)	3381(3)
Si(7)	-306(6)	2773(5)	4100(2)
Si(8)	1556(6)	4358(5)	3623(2)
N(1)	-1205(17)	3582(14)	1420(7)
N(2)	1469(17)	652(14)	1284(6)
N(3)	3778(15)	32(14)	3478(6)
N(4)	1062(15)	2972(13)	3650(7)
C(1)	-4624(25)	4112(28)	1514(16)
C(2)	-2882(34)	3859(26)	354(12)
C(3)	-2498(31)	1591(22)	1330(17)
C(4)	-1692(26)	5270(21)	2296(9)
C(5)	-3028(34)	6431(22)	1124(13)
C(6)	371(24)	5580(19)	1252(10)
C(7)	267(22)	-1364(18)	1971(10)
C(8)	2380(23)	-1937(21)	1005(9)
C(9)	3618(26)	-1577(21)	2061(10)
C(10)	1525(25)	919(20)	26(9)
C(11)	4376(23)	340(22)	760(10)
C(12)	1897(31)	2941(21)	588(11)
C(13)	1865(21)	-1696(18)	3666(9)
C(14)	3747(25)	-1527(26)	4640(11)
C(15)	5223(23)	-2850(21)	3681(10)
C(16)	6568(22)	-669(20)	2767(10)
C(17)	5537(21)	1785(22)	3204(10)
C(18)	6855(25)	-708(21)	4036(12)
C(19)	-59(27)	3140(21)	4821(9)
C(20)	-2231(24)	3736(18)	3800(10)
C(21)	-206(26)	1057(20)	4247(9)
C(22)	-133(24)	5771(18)	3699(9)
C(23)	2448(25)	4887(19)	2918(9)
C(24)	2904(24)	4103(21)	4240(10)

Table 10 Fractional atomic coordinates ( $\times 10^4$ ) for compound 2

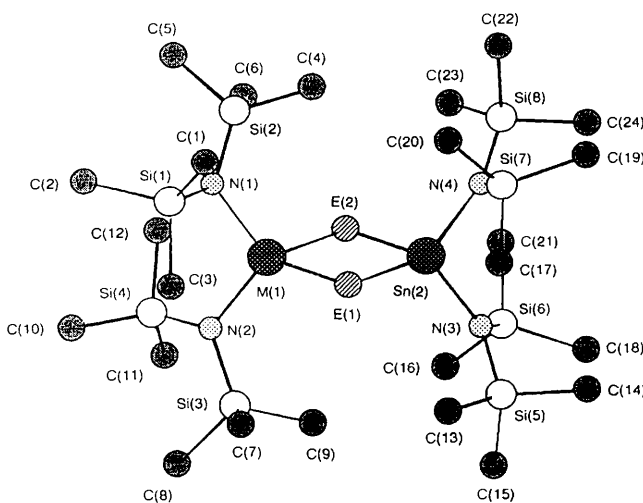
Atom	<i>x</i>	<i>y</i>	<i>z</i>
Sn	999.3(2)	836.6(2)	1334.1(1)
Se	-1926.7(3)	126.0(3)	429.7(2)
Si(1)	-181.4(11)	-1538.7(8)	2443.5(7)
Si(2)	3343.0(10)	524.5(8)	3114.7(7)
Si(3)	693.0(10)	3484.4(8)	2906.6(7)
Si(4)	3657.8(11)	4023.9(8)	1842.7(7)
N(1)	1345(3)	-75(2)	2435(2)
N(2)	1938(3)	2866(2)	2074(2)
C(1)	-2167(4)	-1358(3)	2616(3)
C(2)	-430(5)	-2927(3)	1147(3)
C(3)	291(5)	-2047(4)	3647(3)
C(4)	3691(5)	1916(4)	4425(3)
C(5)	4748(4)	1113(4)	2201(3)
C(6)	3995(5)	-744(4)	3438(4)
C(7)	1924(4)	4973(3)	4134(3)
C(8)	-559(4)	2196(3)	3463(3)
C(9)	-724(4)	3934(3)	2126(3)
C(10)	3192(5)	5443(3)	1640(3)
C(11)	4469(4)	3353(3)	597(3)
C(12)	5358(4)	4742(4)	3046(3)

being smaller than of  $\text{Sn}^{2+}$ , but a steric effect may be a contributory factor. In each of the four compounds 1–4 the N atoms have an approximately trigonal planar environment with the deviation of N from the environment plane ranging between 0.00(0.01) and 0.21(0.01)  $\text{\AA}$ .

In compound 3, the Sn–Te and Sn–N bonds are longer by *ca.* 0.16 and 0.2  $\text{\AA}$ , respectively than the Ge–Te and Ge–N bonds in  $[(\text{Ge}[\text{N}(\text{SiMe}_3)_2]_2(\mu\text{-Te})_2]$  (*cf.* Table 1); likewise, the Te–M–Te angles are wider and the M–Te–M angles narrower in compound 3 ( $\text{M} = \text{Sn}$ ) than in the Ge analogue.<sup>2</sup> As far as the endocyclic bond angles and distances are concerned, the Te or Se parameters are similar in  $[(\text{Ge}[\text{N}(\text{SiMe}_3)_2]_2(\mu\text{-Te})_2]$  and 2, respectively. The compounds  $[(\text{SnBu}')_2(\mu\text{-E})_2]$  ( $\text{E} = \text{S}$ ,  $\text{Se}$  or  $\text{Te}$ ) (*cf.* Table 1), having the similar Bu' ligand at tin, have longer Si–C bonds than the Sn–N bonds of the appropriate com-

**Table 11** Fractional atomic coordinates ( $\times 10^4$ ) for compound 3

Atom	<i>x</i>	<i>y</i>	<i>z</i>
Te(1)	4309.0(8)	3217.2(6)	2499.9(3)
Te(2)	188.5(8)	2306.1(6)	2374.8(3)
Sn(1)	2343.7(7)	3407.8(5)	1745.3(2)
Sn(2)	2219.9(7)	2027.4(5)	3122.2(2)
Si(1)	-156(4)	6209(3)	1723(1)
Si(2)	2998(4)	5928(2)	1053(1)
Si(3)	1889(3)	2463(2)	706(1)
Si(4)	4937(3)	1124(2)	1224(1)
Si(5)	-532(4)	3942(3)	3865(1)
Si(6)	2667(6)	2527(5)	4236(2)
Si(7)	5003(4)	-792(3)	3353(1)
Si(8)	1554(5)	-625(4)	3553(2)
N(1)	1595(9)	5273(6)	1440(3)
N(2)	3226(8)	2387(6)	1149(3)
N(3)	1334(10)	2908(7)	3756(3)
N(4)	3083(9)	154(7)	3387(3)
C(1)	-1950(14)	5667(12)	1750(5)
C(2)	143(17)	6333(12)	2391(5)
C(3)	-669(19)	7844(13)	1330(7)
C(4)	4931(13)	4759(9)	939(5)
C(5)	3480(15)	7119(10)	1363(6)
C(6)	2268(17)	6674(13)	411(5)
C(7)	-67(13)	3630(10)	822(4)
C(8)	2715(15)	2946(11)	40(4)
C(9)	1403(14)	943(9)	747(5)
C(10)	5597(17)	420(11)	617(5)
C(11)	6720(13)	1538(10)	1350(5)
C(12)	4494(13)	-119(9)	1754(5)
C(13)	-2008(14)	4089(11)	3388(5)
C(14)	-360(18)	5563(11)	3847(5)
C(15)	-1554(18)	3382(16)	4516(5)
C(16)	4785(15)	2133(13)	3960(5)
C(17)	2189(31)	839(21)	4696(6)
C(18)	2302(19)	3668(13)	4671(5)
C(19)	6503(13)	-36(12)	2924(5)
C(20)	5168(20)	-2221(11)	3058(6)
C(21)	5775(17)	-1345(14)	4000(5)
C(22)	-415(14)	512(10)	3776(5)
C(23)	1958(20)	-1925(13)	4091(5)
C(24)	1140(22)	-1260(14)	2975(6)

**Fig. 3** Molecular structure of  $[\text{Sn}\{\text{N}(\text{SiMe}_3)_2\}_2(\mu\text{-E})_2\text{M}\cdot\{\text{N}(\text{SiMe}_3)_2\}_2]$  [ $\text{M} = \text{Sn}$ ,  $\text{E} = \text{S } 1$ ,  $\text{Se } 2$  or  $\text{Te } 3$ ;  $\text{M} = \text{Ge}$ ,  $\text{E} = \text{Te } 4$ ], showing the atom labelling scheme. For 2, the two ends of the molecule are related by an inversion centre

pounds 1–3 by *ca.* 0.13–0.20 Å, and the C–Sn–C angles are also wider than the N–Sn–N by *ca.* 2.4–10.3°.<sup>5</sup> The Sn–E bonds in the two series of compounds are of similar dimensions. However, whereas the endocyclic angles and distances for

**Table 12** Fractional atomic coordinates ( $\times 10$ ) for compound 4

Atom	<i>x</i>	<i>y</i>	<i>z</i>
Te(1)	138.1(7)	2313.5(5)	2332.0(2)
Te(2)	4108.9(7)	3253.2(5)	2445.6(2)
Sn	2067.4(7)	2018.3(5)	3096.8(2)
Ge	2259.4(10)	3377.6(7)	1729.0(3)
Si(1)	4857(3)	1109(2)	1254(1)
Si(2)	1842(3)	2442(2)	728(1)
Si(3)	-245(3)	6088(2)	1720(1)
Si(4)	2960(3)	5841(2)	1054(1)
Si(5)	4925(3)	-789(2)	3350(1)
Si(6)	1406(3)	-695(2)	3531(1)
Si(7)	2408(3)	2482(3)	4236(1)
Si(8)	-783(3)	3924(2)	3842(1)
N(1)	3131(8)	2418(6)	1185(3)
N(2)	1531(8)	5095(6)	1436(3)
N(3)	2926(8)	118(6)	3362(3)
N(4)	1132(8)	2878(6)	3740(3)
C(1)	6693(10)	1479(8)	1372(4)
C(2)	4362(11)	-157(8)	1781(4)
C(3)	5538(12)	429(9)	635(4)
C(4)	1355(11)	874(8)	801(4)
C(5)	2740(12)	2897(9)	45(4)
C(6)	-134(11)	3621(9)	820(4)
C(7)	-752(12)	7720(10)	1329(4)
C(8)	4(11)	6217(9)	2388(4)
C(9)	-2101(11)	5594(9)	1749(4)
C(10)	4931(10)	4681(8)	913(4)
C(11)	2281(12)	6653(10)	400(4)
C(12)	3419(11)	6982(9)	1401(4)
C(13)	5566(12)	-1255(10)	4026(4)
C(14)	5214(12)	-2288(9)	3084(4)
C(15)	6427(11)	-30(9)	2933(4)
C(16)	-568(11)	386(8)	3748(4)
C(17)	1824(13)	-2006(10)	4089(4)
C(18)	1099(11)	-1383(8)	2967(4)
C(19)	2075(13)	3749(9)	4635(4)
C(20)	2174(13)	995(10)	4701(4)
C(21)	4541(11)	2264(10)	3937(4)
C(22)	-2200(12)	4043(9)	3361(4)
C(23)	-627(13)	5568(9)	3830(4)
C(24)	-1828(12)	3382(10)	4498(4)

$[\{\text{SnBu}'_2(\mu\text{-S})\}_2]$  are similar to those of compound 1, for  $[\{\text{SnBu}'_2(\mu\text{-Se})\}_2]$  the Sn–Se bonds are shorter by *ca.* 0.1 Å than in compound 2, and for  $[\{\text{SnBu}'_2(\mu\text{-Te})\}_2]$  the Te–Sn–Te angles are wider by *ca.* 3.6–3.7° (and hence the Sn–Te–Sn angles narrower by a similar amount).

The Ge–Te bonds in 4 are longer by *ca.* 0.02 Å compared to those in  $[\{\text{Ge}[\text{N}(\text{SiMe}_3)_2]_2(\mu\text{-Te})\}_2]$ ,<sup>2</sup> while the Sn–Te bonds are *ca.* 0.03 Å shorter than in 3. The Te–Ge–Te angle in 4 is *ca.* 4° wider than in  $[\{\text{Ge}[\text{N}(\text{SiMe}_3)_2]_2(\mu\text{-Te})\}_2]$ , while the Te–Sn–Te angle is *ca.* 3° narrower than in 3.

### Acknowledgements

We are grateful to Dr. A. G. Avent for the NMR spectral data, Lucky-DC Silicone Co., Ltd. (South Korea) for a grant (to E. S. J.), the SERC for support and the Leverhulme Trust for an Emeritus Fellowship for M. F. L.

### References

- Part 16, B. S. Jolly, M. F. Lappert, L. M. Engelhardt, A. H. White and C. L. Raston, *J. Chem. Soc., Dalton Trans.*, 1993, 2653.
- Part 13, P. B. Hitchcock, H. A. Jasim, M. F. Lappert, W.-P. Leung, A. K. Rai and R. E. Taylor, *Polyhedron*, 1991, **10**, 1203.
- P. B. Hitchcock, H. A. Jasim, R. E. Kelly and M. F. Lappert, *J. Chem. Soc., Chem. Commun.*, 1985, 1776.
- M. Wojnowska, M. Noltemeyer, H.-J. Füllgrabe and A. Meller, *J. Organomet. Chem.*, 1982, **228**, 229.
- H. Puff, G. Bertram, B. Ebeling, M. Franken, R. Gattermayer,

- R. Hundt, W. Schuh and R. Zimmer, *J. Organomet. Chem.*, 1985, **379**, 235 and refs. therein.
- 6 P. Brown, M. F. Mahon and K. C. Molloy, *J. Chem. Soc., Chem. Commun.*, 1989, 1621.
- 7 M. J. S. Gynane, D. H. Harris, M. F. Lappert, P. P. Power, P. Rivière and M. Rivière-Baudet, *J. Chem. Soc., Dalton Trans.*, 1977, 2004.
- 8 N. Walker and D. Stuart, *Acta Crystallogr., Sect. A*, 1989, **39**, 158.
- 9 C. K. Fair, MOLEN, An Interactive Intelligent System for Crystal Structure Analysis, User Manual, Enraf-Nonius, Delft, 1990.
- 10 B. Wrackmeyer, *Annu. Rep. NMR Spectrosc.*, 1985, **16**, 73.
- 11 R. W. Chorley, P. B. Hitchcock, M. F. Lappert, W.-P. Leung, P. P. Power and M. M. Olmstead, *Inorg. Chim. Acta*, 1992, **198–200**, 203.

Received 9th May 1995; Paper 5/02925B